MICRO IN-FOCAL CELL STRETCHING PLATFORM WITH PARALLEL PROGRAMMABLE CONTROL

Yuli Huang[1], Nam-Trung Nguyen[1,2]

[1]Nanyang Technological University, Singapore, [2]Mechanobiology Institute, Singapore

ABSTRACT

This paper reports a micro-scale programmable cell stretching platform. The platform keeps the cell monolayer in the microscopic focal plane throughout the stretching process allowing real-time imaging of the cells with magnifications up to 40×, and post-stretching optical analysis with magnification up to 100×. The device consists of highly parallelized stretching array of 15 units with reconfigurable strains. Each unit was an assembly of three elastomeric layers and a bottom glass cover-slip. In the middle of the assembly, an 8 µm thick membrane is used as the stretching substrate for the cells. A programmable pneumatic control system provides actuation. The stretching of the membrane is measured *in situ* using µPIV technique. The results show that a uniform strain of above 60% can be achieved. Preliminary cell stretching experiments in this device with 5 different cell lines were conducted. Both the acute cell deformation and chronic morphological changes in response to the cyclic strain have confirmed the functionality of this platform.

KEYWORDS

Mechanobiology, cell stretcher, pneumatic actuation, BioMEMS, polymeric micromachining.

INTRODUCTION

Mechanical strain is widely used in the study of mechanobiology as a physical stimulus for recreation of microenvironment *in vitro*. In the past two decades, various mechanisms that apply strain to cells have been developed, bringing an increasing possibility for biologists to study physically induced physiological changes. However, most of the conventional mechanisms are meant for bio-chemical assay based bulk analysis. Not until recently was the power of microscopy utilized for obtaining the most direct visualization of these cell behaviors. This paper reports the systematic development of a micro-scale cell stretching platform, which consists of a reconfigurable array of strain units and a highly-parallelized and programmable pneumatic control system. Compared with conventional macro-scale stretchers, the miniaturization of cell culturing chamber has effectively reduced the consumption of cell sample and reagent. The small device footprint allows the implementation of a 3×5 array (every 3 units form a group, which are simultaneously actuated to provide a triplicate experimental condition) on a standard 24 mm×50 mm cover slip. The device is optimized for microscopic imaging. Compared with other stretching mechanisms [2], the platform keeps the cells in microscopic focal plane throughout the stretching process, and hence enables uninterrupted real-time imaging of cells. Furthermore, the reduction of the thickness of the bottom layer allows the device to be used with high resolution immersion-based objective lenses, whose working distance is always limited due to the high numerical aperture. Moreover, the in-plane stretching also ensures the uniformity of the strain inside each unit. As the membrane is actuated sideways, it eliminates the problems of friction and contamination, which is inherent in most post-supporting mechanisms [3-4]. A Labview-based pneumatic control system provides simultaneous switching actuation to 24 stretching units in maximum. The stretching frequency of each 3-unit group can be individually programmed, while the magnitude of strain can be adjusted precisely by setting the vacuum strength to the desired value. To give more test options, a maximum strain of greater than 60% is achieved in this device, compared to that of approximately 30% in most of other mechanisms. Presently, we are also working on the different configurations of the device, Figure 1(d), which would allow different types of strain with desired anisotropicity to be applied to the cells.

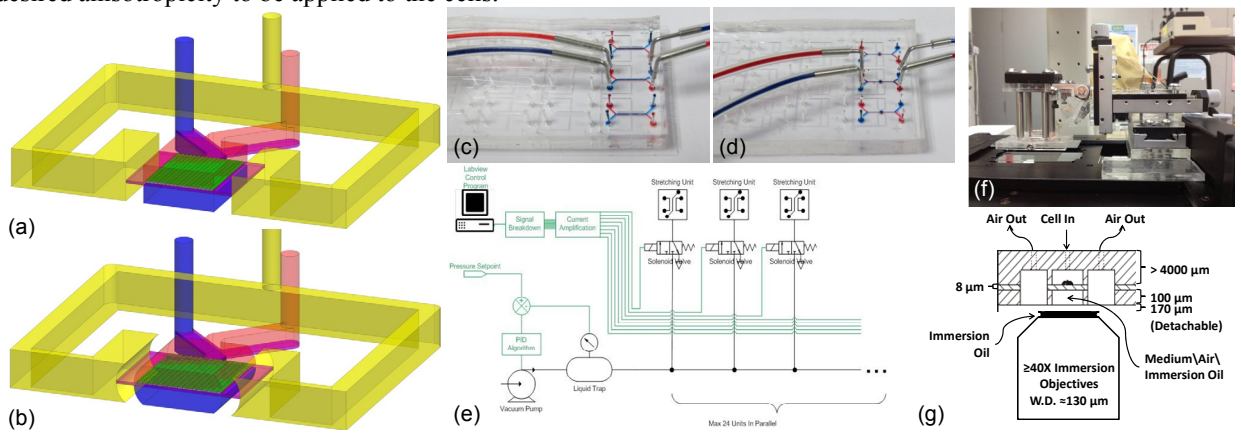

Figure 1. Programmable cell stretching platform: (a-b) Structural concept of uniaxial stretcher at relaxed and stretched state; (c-d) The fabricated platforms of a uniaxial & equibiaxial (underdevelopment) strain array with 3×5 parallelization;(e) Schematics of the pneumatic control system;(f) In-house made 4DOF PDMS alignment and bonding device; (g) Base layer thickness reduction for high-resolution imaging.

978-0-9798064-5-2/µTAS 2012/$20©12CBMS-0001

EXPERIMENTAL

A simplified 2D static structure model of the platform was implemented in ANSYS. Sensitivity analyses about the 4 parameters of interests were carried out, by varying each parameter in iterations. The simulation results suggest that the channel height is the most significant parameter, Figure 2(a). Thus, the channel height is built either with 400 µm for high-strain applications, or 200 µm for best optical compatibility. The simulation also suggests that the strain is linearly proportional with the vacuum strength. The model predicted a uniform strain on the membrane ensuring all cells loaded in one unit experiencing the identical physical condition.

Both the top and bottom elastomeric layer were fabricated by PDMS replica molding. However, the bottom layer is casted with an additional step of pressing a cover-slip down onto the PDMS (under a pressure of 40 Pa), until it is firmly in contact with the SU8 mold. The PDMS formed a reversible bond with the cover-slip allowing post-stretching microscopic analysis with higher magnification objectives. Both the SU8 master-mold and a glass-slide were pre-treated with Teflon (STS Deep RIE, 1 min). PDMS was cured at room temperature for 48 hours to avoid thermal expansion. The middle PDMS membrane is spin-coated at a rate of 4000 rpm for 180 sec on a circular acrylic disk, to form a layer of 8±1 µm. This membrane is bonded with the bottom layer first on the cover-slip with oxygen-plasma treatment (120W @30s, NT-2, BSET EQ). The bonded structure is plasma treated again with the upper layer before they are aligned and bonded. To carry out the bonding process with both rapidity and precision, a special in-house made 4 DOF alignment tool was used together with a microscope, Figure 1(f). To connect the two half vacuum channels, the excessive membrane is either mechanically torn off or etched (TBAF:DMF, 3:1, v/v). Each vacuum chamber is flushed by the etchant at a rate of 100 µl/min, which usually takes 15 min to completely etch away the 8 µm membrane. To clean the residue of etchant, the vacuum chamber is further flushed by DMF and ethanol consecutively, for 10 minutes each at the same flow-rate.

The control system is depicted in Fig. 1(e), the negative pressure is supplied by a vacuum pump (Dryfast 2034, Welch), and is maintained at an exact pressure in the range of 20~760 Torr by a vacuum controller (LabAid 1640, Welch). The vacuum output branches into 3 manifolds, and was further divided into 24 ports. Each port is regulated by a solenoid valve (S10MM-31-12-3, pneumadyne). A custom control program and signal translation circuit was used for generating electric signals, which simultaneously actuate the valves with different frequencies up to 100Hz. The resultant strain in the device is qualitative characterized with cross-correlation algorithm (OpenPIV). Fluorescent micro-beads (diluted in ethanol to 0.25%) were coated onto the membrane prior to bonding with the bottom layer. To give a quantitative interpretation of the strain distribution on different locations of the membrane, sequential recording were taken at discrete vacuum levels from 20 to 720 Torr, with an increment of 100 Torr. The displacement of each particle was manually measured (ImageJ) for determining the strain.

The cell channel was cleaned and coated with collagen-gel solution in the way reported by Huh et al.[1]. After 2 hours of coating, the channel was rinsed again by the respective cell growth medium, and cells trypsinized and resuspended at the concentration of 3~5 millions/ml. Only 10 µl cells were taken by the pipette tip for one unit. One pipette tip was inserted into the channel inlet, while another empty pipette tip was inserted in the outlet to gently redraw 5 µl. The device was incubated for 1~3 hours until cells attach to the membrane. Subsequently, the pipette tips were removed. Tubing was connected to the two ends of the channel to supply nutrient to the cells. The whole setup is housed in a mini incubator (5% CO_2, 37˚C and high humidity) on the microscope stage.

Five different cell lines including A549, COS7, PTK2, RBL and benign human foreskin fibroblast (Fibro) were cultured in the devices following the above protocol. Real-time video were recorded at 5 fps to determine the immediate cell shape distortion in response to the applied strain. A relatively small constant cyclic strain (5%, 0.1 Hz) was applied to the cells to investigate the strain-induced morphological changes. The test with each cell line is triplicate and compared with control, i.e. each cell line is cultured simultaneously in 6 units, 3 of them are stretched under the identical condition while 3 others were not stretched. 40× magnification multi-stage time-lapsed recordings were taken for all samples for more than 6 consecutive hours, at an interval of 5 min. After the stretching, the cells were fixed in the device with formaldehyde (4%), and subsequently permeablized by cold acetone (-20˚C). Immunofluorescence staining was applied to 3 major cytoskeleton components, namely actin-filament, micro-tubule and nucleolus.

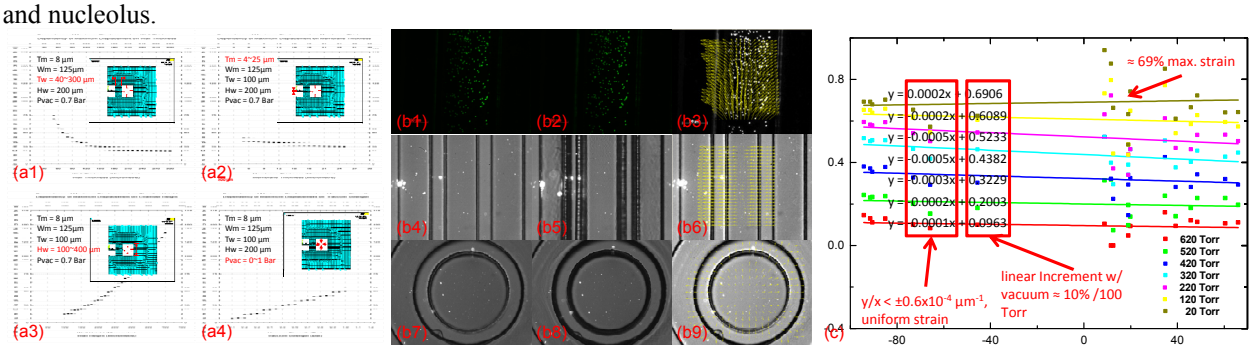

Figure 2 Characterization and experiments: (a) The sensitivity of resultant strain to the variation of geometric parameters and vacuum strength; (b) Qualitative analysis of deformation\strain using cross-correlation algorithm for (b1) beads suspended in liquid flowing in a uniaxial stretching unit, (b2) beads embedded in membrane in a uniaxial and (b3) equibiaxial stretching unit, respectively; (c) Strain distribution on the membrane at discrete vacuum levels.

RESULTS AND DISCUSSION

Stretching in uniaxial or equibiaxial direction can be quantitatively visualized. The displacement increases linearly from zero at the centreline\centre to the maximum at the membrane edge. The linear proportionality means strain uniformity. The linear dependency between the vacuum strength and strain, as predicted by the simulation, is also confirmed by quantitative results.

By comparing the stretched and relaxed state of an isolated cell in the real-time video recording, we observed that cells have formed firm bonding with the membrane, and hence following the motion of the membrane precisely. On the other hand, the time lapse recording of three different cell lines demonstrated the various cell activities in live, including migration, spreading, contraction, blebbing, etc. Comparison with controls (images not shown) suggests that the RBL cells become especially active under such stretching regimen, while the PTK2 cells are relatively insensitive to this level of stretching. Hypothetical merging of cells has also been observed in A549, although the real conclusion can only be drawn after systematic studies. After immunofluorescence staining, a 2D confocal image of the PTK2 cells were taken at 100× magnification with the bottom cover-slip of the device detached. By detaching the bottom coverslip, the stretcher has obtained an ultra thin bottom, of a thickness slightly above 100 µm. Either cell culture medium or immersion oil can be injected into the bottom half cell channel to match the reflective index, allowing the use of advanced microscopy.

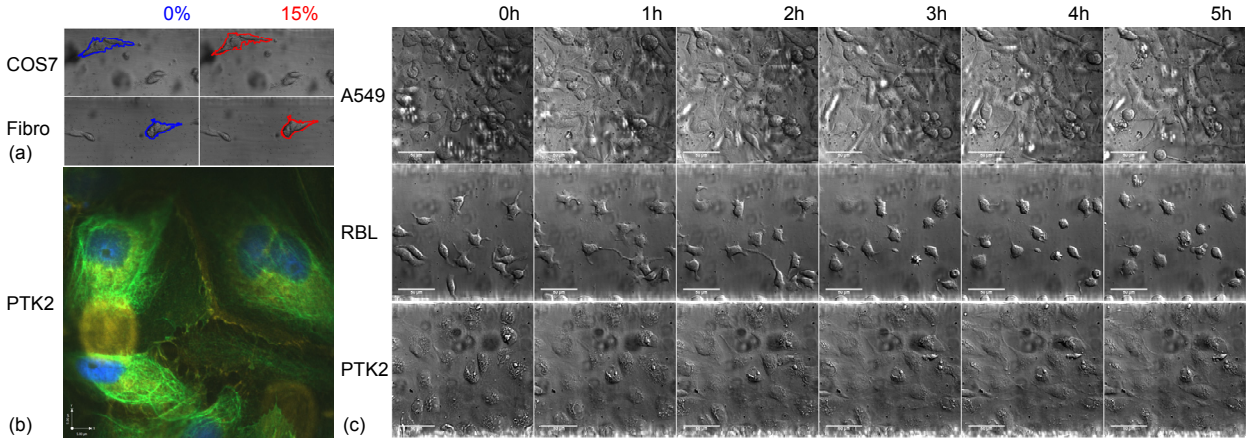

Figure 3. Cell stretching experiments: (a) Snapshots of relaxed and stretched state taken from real-time video recording of isolated cells, for the analysis of cell shape distortion in response to the stretching the membrane (15%,1Hz); (b) Confocal microscopy image of PTK2; (c) Time lapse recording of 3 cell-lines subjected to cyclic stretching (5%, 0.1Hz), with 40× Differential Interference Contrast (DIC) microscopy. Multi-stage time-lapse recordings were taken at 5 min interval.

CONCLUSIONS

In this platform, a side-stretching mechanism is utilized for keep cell stretching in focal-plane. By successfully reducing the distance between the stretching membrane and bottom, this platform can provide a superior optical property that is essential for utilizing the power of advanced microscopy for mechanobiological studies. Meanwhile, the high parallelization, realized by having individually programmable stretching regimens and downscaling of form factors, will also significantly increase the experimental throughput.

The authors would like to acknowledge the generous funding from Mechanobiology Institute, Singapore. We thank Micheal Sheetz for initiating this project. We are also grateful to the advices from Leyla Kocgozlu, Benoit Ladoux on the device modification, assistance from Lok Khoi Seng, Lee Peng Foo for the biological experiments and support from Su Maohan as well as Wu Min for microscopic imaging.

REFERENCES

[1] Huh, D., B.D. Matthews, A. Mammoto, M. Montoya-Zavala, H.H. Yuan, D.E. Ingber, *Reconstituting organ-level lung functions on a chip*. 2010, Science, 2010, 328(5986), p. 1662-1668.

[2] Shimizu, K., A. Shunori, K. Morimoto, M. Hashida, S. Konishi, *Development of a biochip with serially connected pneumatic balloons for cell-stretching culture*, Sensors and Actuators, B: Chemical, 2011. 156(1): p. 486-493.

[3] Moraes, C., J. H. Chen, Y. Sun, C. A. Simmons, *Microfabricated arrays for high-throughput screening of cellular response to cyclic substrate deformation*. Lab on a Chip - Miniaturisation for Chemistry and Biology, 2010. 10(2), p. 227-234.

[4] Simmons, C. S., J.Y. Sim, P. Baechtold et al., *Integrated strain array for cellular mechanobiology studies*. Journal of Micromechanics and Microengineering, 2011. 21(5), p. xxx-xxx.

CONTACT

Nam-Trung Nguyen; Tel: +65 67904457; mntnguyen@ntu.edu.sg; http://www.ntu.edu.sg/home/mntnguyen